Surface Science 603 (2009) L95–L98

Contents lists available at ScienceDirect

Surface Science

journal homepage: www.elsevier.com/locate/susc

Surface Science Letters

Friction between α-Al_2O_3(0 0 0 1) surfaces and the effects of surface hydroxylation

Dongshan Wei [a], Yanhang Zhang [a,b,*]

[a] Department of Mechanical Engineering, Boston University, Boston, MA 02215, United States
[b] Department of Biomedical Engineering, Boston University, Boston, MA 02215, United States

ARTICLE INFO

Article history:
Received 10 February 2009
Accepted for publication 30 June 2009
Available online 5 July 2009

Keywords:
Molecular dynamics
Friction
Alumina
Surface hydroxylation

ABSTRACT

Molecular dynamics simulations were performed to study the friction between hydroxylated α-Al_2O_3(0 0 0 1) surfaces at the temperature of 300 K. Effects of the degree of surface hydroxylation and sliding velocity have been discussed. Results indicate that the friction coefficient decreases with increased degrees of hydroxylation. For all degrees of surface hydroxylation, the friction law crosses over from thermal activation to viscous damping at sliding velocity of 80 m/s.

As micro- and nano-scale devices continue to develop and evolve it is increasingly important to control the surface properties and device interaction with its surrounding environment. Thin film coatings have been applied to numerous microelectromechanical systems (MEMS) structures for optical application, insulation, biocompatibility, anti-stiction, wear and corrosion inhibition, etc. through a variety of chemical surface modification processes. The application and commercialization of MEMS devices suffers from reliability problems, many of which are due to the friction and wear between the moving parts. Recent studies have demonstrated that a nano-scale Al_2O_3 layer deposited by atomic layer deposition (ALD) yields a hard and protective conformal coating that significantly reduces the abrasive wear in MEMS [1,2].

Alumina surfaces are easily hydroxylated due to the ready reaction between alumina and water molecules in air and solution environments. The reaction between the outermost Al atoms and the adsorbed water leads to dissociation of water molecules. The protonated H atoms then react with the exposed O atoms to form hydroxyls [3,4]. Hydroxylation can influence the structure and stability of the outmost layer of Al_2O_3 crystal [5]. Friction between alumina surfaces has been studied experimentally using surface force apparatus (SFA) [6,7] and tribometer [8]. Using MD simulations, many basic problems at the atomic scale such as friction coefficient [9], friction law [10], interfacial interaction [11], temperature gradients and energy dissipation during sliding [12,13] have been addressed. However, all of these experimental and simulation studies on friction of alumina have been focused on bare and fully hydroxylated surfaces. Partially hydroxylated alumina surfaces exist under low-pressure conditions and have significantly different adhesion and nucleation density compared with fully hydroxylated ones [14,15]. Detailed investigations of friction between partially hydroxylated alumina surfaces are not currently available.

In micro- and nano-scale, without the presence of chemical and/or environmental adhesion across the interface, friction law that friction force F_x is in logarithmic dependence on sliding velocity v_s can be safely drawn [16] and has been demonstrated in studies of tip-surface [17–20] contacts. But considering wider sliding velocity ranges, previous studies have shown that the dependence of F_x on v_s has a crossover. Crossovers between logarithmic and linear dependence [21–23], logarithmic and power law dependence [22,23], and velocity-independence and linear dependence [23,24] have been shown. Interested readers are referred to Szlufarska et al. [16] for detailed reviews on the velocity dependence of friction force.

In this letter, we studied the friction between α-Al_2O_3(0 0 0 1) surfaces at the temperature of 300 K using MD simulations. Effects of the degree of hydroxylation p on the friction and dependence of F_x on v_s are discussed in detail. In MD simulations, an interaction potential including two- and three-body terms [25,26] is used to describe the van der Waals (vdW), Coulombic, and bonding interactions between Al, O, and H atoms. This interaction potential was used to simulate the alumina crystals and surfaces. The calculated structures of bulk crystals, surface energy, and surface relaxation of alumina were shown to be in excellent agreement with experimental results [25]. It was also properly applied to describe the silica/alumina interface interaction [26,27], in which the silica/

* Corresponding author. Address: Department of Mechanical Engineering, Boston University, 110 Cummington Street, Boston, MA 02215, United States. Tel.: +1 617 358 4406; fax: +1 617 353 5866.
E-mail address: yanhang@bu.edu (Y. Zhang).

0039-6028/$ - see front matter © 2009 Elsevier B.V. All rights reserved.
doi:10.1016/j.susc.2009.06.022

alumina interface formation by a sol–gel transition and the anisotropic dissolution of alumina surface into silicates had been well simulated. Very recently, a new interaction potential for alumina has been proposed to account for the effect of charge-induced dipole interaction [28], however the parameters for H atoms are not currently available.

To construct the sliding model, α-Al_2O_3(0 0 0 1) surface is generated via cleaving and relaxing the bulk crystal of α-Al_2O_3, comprised of $6 \times 6 \times 1$ unit cells with a volume of $6a \times 3\sqrt{3}a \times 1c$, where a and c are crystal cell parameters with $a = 4.76$ Å and $c = 12.99$ Å at 300 K. A fully hydroxylated surface is constructed by removing the outmost layer Al atoms and adding H atoms to the exposed O atoms in each unit cell, which results in 108 H atoms, 396 Al atoms, and 648 O atoms included in the fully hydroxylated surface. A partially hydroxylated surface is formed by placing hydroxylated unit cells and bare unit cells side-by-side in a ratio [15]. A mirror image of the generated α-Al_2O_3(0 0 0 1) is used to create a bottom surface at a given distance which is much greater than the cutoff radius of the interactions. To make the two surfaces contact, a compression process is conducted by moving the top surface down slowly. After each movement, the system is equilibrated with a MD run of at least 50 ps. The sliding simulation is carried out at a constant separation D between the outermost Al–O_3–Al layers of the top and bottom surfaces. The atoms in the outermost Al–O_3–Al layer of the top surface are given a constant sliding velocity, v_s, in the x direction and are kept fixed in the y- and z-directions, while the atoms in the outermost layer of the bottom surface are kept fixed in all directions [10,29]. A snapshot of the sliding simulation is shown in Fig. 1. The lateral dimensions of the sliding system are 28.6 Å × 24.7 Å with periodic boundary conditions in the x- and y-directions. A vacuum layer of 15 Å is inserted along the z-direction to avoid the interaction between outermost layers of the two surfaces. Berendsen thermostat is implemented to Al–O_3–Al atoms next to the outermost layers. A cutoff distance of 5.5 Å for the two-body interactions [25,26] and a time step of 0.25 fs and are used in all simulations. Since separation D between the two surfaces is kept at constant, the normal force has a slight fluctuation of ±5% during sliding. The friction force F_x and the normal force F_z discussed below are average forces of all atoms in the top surface in x- and z-directions, respectively [10,29]. For each sliding simulation, only one configuration is used. The top surface slides at least 20 Å to assure enough statistical data.

Fig. 2 shows the relationships between the friction force F_x and the normal force F_z for α-Al_2O_3(0 0 0 1) surfaces with different degrees of hydroxylation. For $p = 0\%$ and 100%, a linear relation of $F_x = \alpha A + \mu F_z$ can be used to fit the data, where μ is the friction coefficient, A is the surface area and α is a constant under a given degree of hydroxylation. The fitting results give $\mu = 0.12$ for $p = 0\%$ and $\mu = 0.039$ for $p = 100\%$. We can see that the friction coefficient prominently decreases when the alumina surface is fully hydroxylated. The reason for the decrease of the friction coefficient mainly comes from reduced interfacial interaction (Coulombic and vdW interactions) due to the substitution of the weak attraction between H and O for the strong attraction between Al and O at the interface. Lodziana et al. [5] have shown that hydroxylation greatly lowers the surface energy of α-Al_2O_3 surface. Previous MD simulations of friction between alumina surfaces with different surface potentials have shown that weaker interfacial interaction can lead to lower friction coefficient [11]. Similar results have also been shown in studies of friction between diamond-like carbon films with hydrogen termination [30]. In addition, the friction coefficient of $\mu = 0.12$ between the bare alumina surfaces is within the range of experimental measurements, from 0.08 to 0.15, for smooth Al_2O_3 surfaces [7,8]. For the fully hydroxylated alumina surfaces, no experimental results are currently available. Our result of $\mu = 0.039$ is smaller than the simulation result of $\mu = 0.14$ from Mann and Hase [9]. This discrepancy might due to the differences in potential energy function. The Coulombic interaction between atoms was not included in their wok.

For partially hydroxylated surfaces with $p = 33.3\%$, 50%, and 66.7%, the linear relationship between F_x and F_z does not appear until the normal force greater than a threshold value of F_c. The nonlinear behavior at $F_z < F_c$ may result from the increased surface roughness due to partial hydroxylation. We calculated the atomic-scale roughness σ before sliding as $\sigma = \sqrt{\langle\langle z(x,y)^2\rangle - \langle z(x,y)\rangle^2\rangle}$, where $z(x, y)$ is the distance of an area of 2 Å × 2 Å at position (x, y) from the geometric center of the surface, and the outer angle brackets indicates an average over areas [31]. For $p = 0\%$, 33.3%, 50%, 66.7%, and 100%, σ is 0.1, 0.9, 0.8, 0.5, and 0.2 Å, respectively. The atomic-scale roughness of partially hydroxylated surfaces is higher than those of the bare surface and fully hydroxylated surfaces. The increased roughness of partially

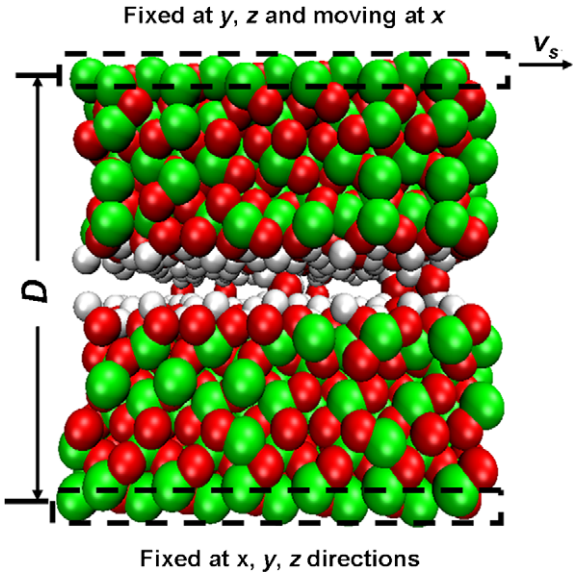

Fig. 1. A snapshot of the sliding simulation at initial time with $p = 100\%$: red, O; green, Al; and gray, H. (For interpretation of the references in colour in this figure legend, the reader is referred to the web version of this article.)

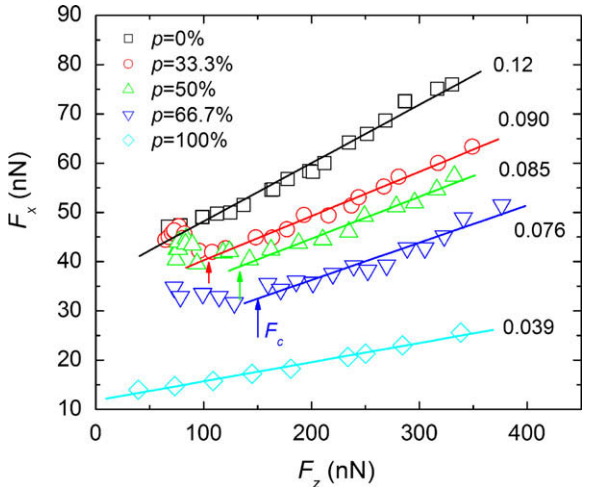

Fig. 2. Relationship between friction force F_x and normal force F_z for α-Al_2O_3 surfaces at $v_s = 200$ m/s with different degrees of hydroxylation (p). The solid lines are linear fits and the friction coefficients are given. For $p = 33.3\%$, 50%, and 66.7%, linear fits are on data when F_z is greater than F_c indicated by arrows.

SURFACE SCIENCE LETTERS

hydroxylated surfaces might increases the normal force necessary to bring the surfaces into contact and thus leads to the initial independent relationship between F_x and F_z. Although the potential we used cannot describe the chemical reactions, tribochemical effects at the interface such as wear can also lead to independent relationship between F_x and F_z under lower normal forces [32].

To obtain the friction coefficient for partially hydroxylated surfaces, the curves after $F_z > F_c$ were linearly fitted. In Fig. 3, the variation of friction coefficient with the degree of hydroxylation is presented for different sliding velocities. At the same sliding velocity, friction coefficient decreases with increased degree of hydroxylation. This trend is in agreement with the MD simulation results of partially hydrogen-terminated carbon surfaces [32], in which the reduced adhesion due to the substitution of weak C–H bonding interaction for the strong C–C bonding interaction leads to a decrease of friction coefficient. Friction coefficient has been shown to be proportional to the square of the surface corrugation [33,34]. However in our study, both the surface roughness and composition change as the degree of hydroxylation varies. For hydroxylated surfaces, despite surface roughness increases in comparison with the bare surface, our simulations consistently show friction coefficient decreases with the increase of the degree of hydroxylation. These results imply that the weakened attractive interaction between surfaces due to hydroxylation plays a dominant role in changing the friction coefficient. Previous studies have also shown that the orientation of the terminal groups at the interface have a significant impact on friction [35,36]. Here we also noticed that both the average and standard deviation of the orientation angle between the O–H bond vector and the normal (z-) direction of the hydroxylated alumina surface before sliding increase when the degree of hydroxylation decreases. This wide-range distribution of the orientation angles might correlate with the higher friction coefficient at low hydroxylation. In addition, results in Fig. 3 indicate that the friction coefficient increases with the sliding velocity, and the trend is slightly more significant for the partially hydroxylated surfaces.

In Fig. 4a, the relationships between friction force and sliding velocity under different normal forces are shown. The friction force F_x increases with the sliding velocity v_s; a prominent linearity appears at $v_s > 80$ m/s. In Fig. 4b F_x versus log v_s are plotted for various degrees of hydroxylation. At $v_s < 80$ m/s, F_x shows a linear dependence on log v_s for all alumina surfaces. This logarithmic dependence has been observed experimentally from tip-surface friction study and derived using reaction rate theory based on the Tomlinson model [18]. At lower sliding velocities, thermal fluctuation is important to induce stick-slip motion [37], which results in a logarithmic dependence of friction on sliding velocity [38]. When the sliding velocity $v_s \approx 80$ m/s, this trend starts to change. At $v_s > 80$ m/s, F_x shows a linear dependence on v_s, as shown in Fig. 4b by the dash lines. At higher sliding velocities, the thermal activation becomes less important and the stick-slip motion of interfacial atoms is replaced by viscous damping motion, which gives rise to a viscous friction [24]. Viscous friction between solid surfaces has been explained as the anharmonic coupling of phonons at the interface [39]. Recent study on simulation of friction between α-Al_2O_3 surfaces also shows that viscous friction occurs at high sliding velocity, where the motion of interfacial atoms is damped by excited phonons and is not controlled by the static interfacial energy barrier [10]. However to understand the mechanisms that cause the crossover for hydroxylated α-Al_2O_3 surfaces, detailed studies on the dynamics of kinetic friction and energy dissipation during the sliding need to be performed [24,40].

In conclusion, we report the influences of hydroxylation on the friction properties of α-Al_2O_3(0 0 0 1) surfaces using MD simulations. Hydroxylation reduces the friction coefficient of alumina surfaces despite it increases the atomic-scale roughness of surface. The friction coefficient has a slight increase with the sliding veloc-

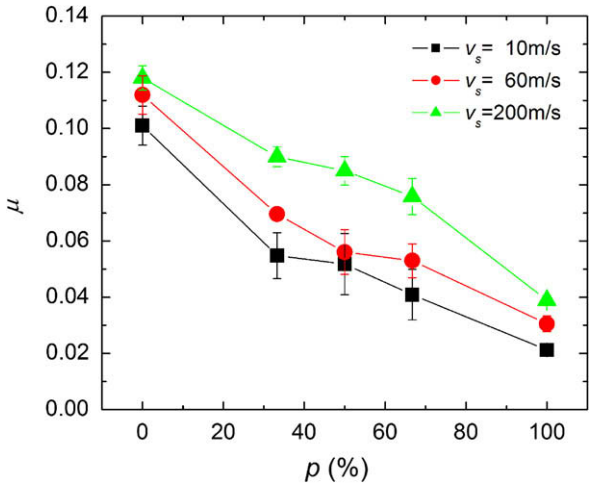

Fig. 3. Variation of friction coefficients with the degree of hydroxylation at different sliding velocities.

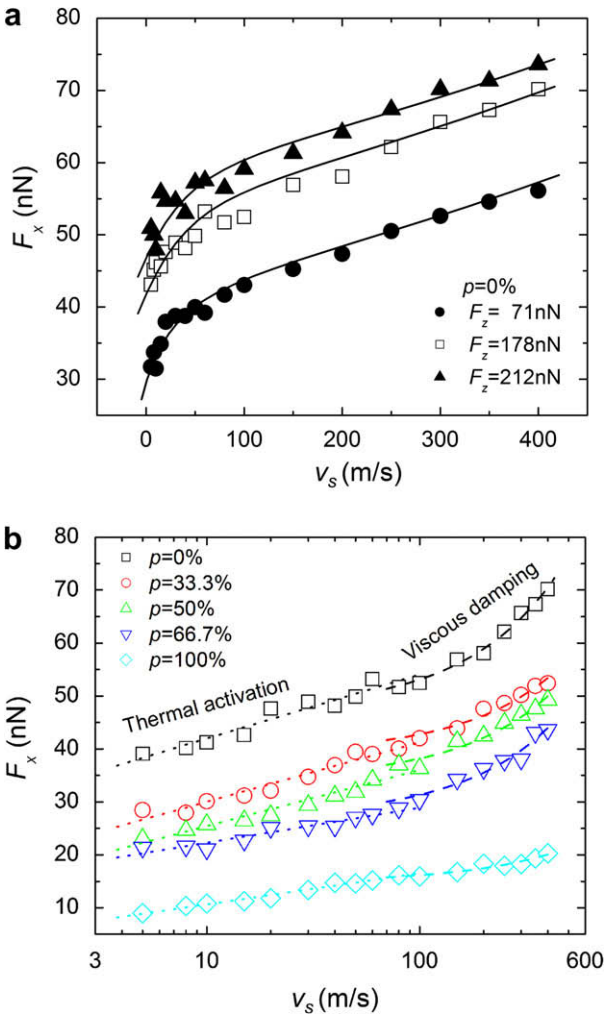

Fig. 4. (a) Sliding velocity v_s dependence of friction force F_x under various normal forces for bare aluminum surface under different normal forces; (b) semi-logarithm plots of friction force versus sliding velocity for different degrees of hydroxylation under normal force $F_z = 170 \pm 8$ nN. The solid lines are for viewing guidance. The dotted lines and the dash lines are linear fittings of F_x versus log v_s and F_x versus v_s, respectively.

ity within the velocity range we studied. The sliding velocity dependence of the friction force is observed to have a crossover at $v_s \approx 80$ m/s. The simulation results explain the roles of surface hydroxylation on the friction behavior of metal oxide surfaces and confirm recent experimental findings of the dependence of friction force on sliding velocity. In spite of the discrepancy with experimental SFA studies in time and size scales, MD simulations give convincing results about the friction properties between the hydroxylated alumina surfaces.

Acknowledgements

The authors would like to acknowledge the funding support by the Young Faculty Award from DARPA/MTO (W911NF-07-1-0181). The authors are thankful for the thoughtful discussions with Professor Feng Wang and the computational support from the Scientific Computing and Visualization (SCV) Center and the Biomedical Engineering Computational Simulation Facility at Boston University.

References

[1] N.D. Hoivik, J.W. Elam, R.J. Linderman, V.M. Bright, S.M. George, Y.C. Lee, Sens. Actuators A: Phys. 103 (2003) 100.
[2] T.M. Mayer, J.W. Elam, S.M. George, P.G. Kotula, R.S. Goeke, Appl. Phys. Lett. 82 (2003) 2883.
[3] J.M. Wittbrodt, W.L. Hase, H.B. Schlegel, J. Phys. Chem. B 102 (1998) 6539.
[4] K.C. Hass, W.F. Schneider, A. Curioni, W. Andreoni, Science 282 (1998) 265.
[5] Z. Lodziana, J.K. Norskov, P. Stoltze, J. Chem. Phys. 118 (2003) 11179.
[6] Z.H. Xu, W. Ducker, J. Israelachvili, Langmuir 12 (1996) 2263.
[7] A. Berman, S. Steinberg, S. Campbell, A. Ulman, J. Israelachvili, Tribol. Lett. 4 (1998) 43.
[8] D.H. Hwang, K.H. Zum Gahr, Wear 255 (2003) 365.
[9] D.J. Mann, W.L. Hase, Tribol. Lett. 7 (1999) 153.
[10] Q. Zhang, Y. Qi, L.G. Hector Jr., T. Cagin, W.A. Goddard III, Phys. Rev. B 72 (2005) 045406.
[11] D.J. Mann, L. Zhong, W.L. Hase, J. Phys. Chem. B 105 (2001) 12032.
[12] H.W. Xie, K.Y. Song, D.J. Mann, W.L. Hase, Phys. Chem. Chem. Phys. 4 (2002) 5377.
[13] O.A. Mazyar, H.W. Xie, W.L. Hase, J. Chem. Phys. 122 (2005).
[14] J.A. Kelber, Surf. Sci. Rep. 62 (2007) 271.
[15] R. Meyer, J. Lockemeyer, R. YeateS, M. Lemanski, D. Reinalda, M. Neurock, Chem. Phys. Lett. 449 (2007) 155.
[16] I. Szlufarska, M. Chandross, R.W. Carpick, J. Phys. D: Appl. Phys. 41 (2008) 123001.
[17] T. Bouhacina, J.P. Aim, S. Gauthier, D. Michel, V. Heroguez, Phys. Rev. B 56 (1997) 7694.
[18] E. Gnecco, R. Bennewitz, T. Gyalog, C. Loppacher, M. Bammerlin, E. Meyer, H.J. Güntherodt, Phys. Rev. Lett. 84 (2000) 1172.
[19] S. Sills, R.M. Overney, Phys. Rev. Lett. 91 (2003) 095501.
[20] S. Andre, J. Lars, H. Hendrik, F. Harald, Appl. Phys. Lett. 88 (2006) 123108.
[21] F. Heslot, T. Baumberger, B. Perrin, B. Caroli, C. Caroli, Phys. Rev. E 49 (1994) 4973.
[22] M.H. Müser, Phys. Rev. Lett. 89 (2002) 224301.
[23] N.S. Tambe, B. Bhushan, Nanotechnology 16 (2005) 2309.
[24] O. Zwörner, H. Hölscher, U.D. Schwarz, R. Wiesendanger, Appl. Phys. A 66 (1998) S263.
[25] S. Blonski, S.H. Garofalini, Surf. Sci. 295 (1993) 263.
[26] S. Blonski, S.H. Garofalini, J. Phys. Chem. 100 (1996) 2201.
[27] Glenn K. Lockwood, S. Zhang, S.H. Garofalini, J. Am. Ceram. Soc. 91 (2008) 3536.
[28] V. Priya, K.K. Rajiv, N. Aiichiro, R. Jose Pedro, J. Appl. Phys. 103 (2008) 083504.
[29] J.A. Harrison, R.J. Colton, C.T. White, D.W. Brenner, Wear 168 (1993) 127.
[30] H. Ronkainen, K. Holmberg, in: C. Donnet, A. Erdemir (Eds.), Tribology of Diamond-Like Carbon Films: Fundamentals and Applications, Springer, New York, 2008, p. 155.
[31] S.P. Adiga, P. Zapol, L.A. Curtiss, J. Phys. Chem. C 111 (2007) 7422.
[32] G.T. Gao, P.T. Mikulski, J.A. Harrison, J. Am. Chem. Soc. 124 (2002) 7202.
[33] M. Cieplak, E.D. Smith, M.O. Robbins, Science 265 (1994) 1209.
[34] T. Coffey, J. Krim, Phys. Rev. Lett. 95 (2005) 076101.
[35] P.T. Mikulski, G. Gao, G.M. Chateauneuf, J.A. Harrison, J. Chem. Phys. 122 (2005) 024701.
[36] P.T. Mikulski, L.A. Herman, J.A. Harrison, Langmuir 21 (2005) 12197.
[37] A. Schirmeisen, L. Jansen, H. Fuchs, Phys. Rev. B 71 (2005) 245403.
[38] Y. Sang, M. Dub, M. Grant, Phys. Rev. Lett. 87 (2001) 174301.
[39] E.D. Smith, M.O. Robbins, M. Cieplak, Phys. Rev. B 54 (1996) 8252.
[40] A. Schirmeisen, H. Holscher, Phys. Rev. B 72 (2005) 045431.